Dual Roles of Graphene Oxide in Chondrogenic Differentiation of Adult Stem Cells: Cell-Adhesion Substrate and Growth Factor-Delivery Carrier

*Hee Hun Yoon, Suk Ho Bhang, Taeho Kim, Taekyung Yu, Taeghwan Hyeon, and Byung-Soo Kim**

Here, it is shown that graphene oxide (GO) can be utilized as both a cell-adhesion substrate and a growth factor protein-delivery carrier for the chondrogenic differentiation of adult stem cells. Conventionally, chondrogenic differentiation of stem cells is achieved by culturing cells in pellets and adding the protein transforming growth factor-β3 (TGF-β3), a chondrogenic factor, to the culture medium. However, pellets mainly provide cell-cell interaction and diffusional limitation of TGF-β3 may occur inside the pellet both of these factors may limit the chondrogenic differentiation of stem cells. In this study, GO sheets (size = 0.5–1 μm) were utilized to adsorb fibronectin (FN, a cell-adhesion protein) and TGF-β3 and were then incorporated in pellets of human adipose-derived stem cells (hASCs). The hybrid pellets of hASC-GO enhanced the chondrogenic differentiation of hASCs by adding the cell-FN interaction and supplying TGF-β3 effectively. This method may provide a new platform for stem cell culture for regenerative medicine.

1. Introduction

Graphene (G) and its derivatives are being explored for use in various biomedical applications such as drug delivery,[1] imaging,[2] and photothermal cancer therapy.[3,4] Furthermore, studies are expanding in the field of regenerative medicine, because these materials are capable of influencing cellular behaviors such as the adhesion,[5] growth,[5] and differentiation of stem cells.[5–8] It was reported that G induced the osteogenesis of human mesenchymal stem cells (hMSCs)[5] and the differentiation of human neural stem cells into neurons,[6] while graphene oxide (GO) induced differentiation of hMSCs to adipocytes[5] and myoblasts.[7] The previous studies indicate that G and GO have distinct properties when utilized as substrates for stem cell culture and differentiation. For example, GO showed higher protein adsorption compared with G.[5] Although they both enhanced cell adhesion and growth, proteins such as insulin interacted with G and GO in different manners.[5] GO formed an electrostatic interaction with insulin and preserved the protein structure, while G denatured the native structure. Because the insulin protein structure was preserved on GO, the adipogenic differentiation of hMSCs was significantly enhanced when cultured on GO compared with G.[5] Although many studies have explored how various properties of G and GO differentiate adult stem cells,[5–8] there has been no report on the use of G or GO for chondrogenic differentiation. This study reports, for the first time, the use of GO for the chondrogenic differentiation of stem cells.

The chondrogenic differentiation of adult stem cells is conventionally achieved through the culture of cells in pellets.[9] Cell condensation into pellets mimics the chondrogenic progenitor cell derivation during embryogenesis through cell condensation.[10] However, because the major composition of the pellets is cells and the extracellular matrix (ECM) amount is negligible, the cell-ECM interaction that promotes chondrogenic differentiation[11] is absent. Additionally, the diffusional limit of approximately 150 – 200 μm restricts the mass transportation of many molecules, including oxygen, into the pellets.[12] Such characteristics thus limit the size of the pellets because pellets larger than the diffusional limit display a necrotic core surrounded by a viable cell layer. To overcome such hurdles, we used GO sheets as both a cell-adhesion substrate and a chondrogenic inducer-delivery carrier for in vitro chondrogenic differentiation of human adipose-derived stem cells (hASCs) in pellets in this study (**Figure 1**). GO sheets (size = 0.5–1 μm) were utilized to adsorb fibronectin (FN, a cell-adhesion protein) and transforming growth factor-β3 (TGF-β3) (a chondrogenic inducer) and were then incorporated into hASC pellets. The adsorption of FN and TGF-β3 on GO sheets relies on the surface chemistry of GO. GO features both hydrophobic π domains

H. H. Yoon,[+] T. Kim, Prof. T. Hyeon, Prof. B.-S. Kim
School of Chemical and Biological Engineering
Seoul National Univeristy
Seoul 151–744, Republic of Korea
E-mail: byungskim@snu.ac.kr
S. H. Bhang[+]
School of Chemical Engineering
Sungkyunkwan University
Suwon 440-746, Republic of Korea
T. Yu
Department of Chemical Engineering
Kyung Hee University
Yongin 446-701, Republic of Korea
[+]These authors contributed equally.

DOI: 10.1002/adfm.201400793

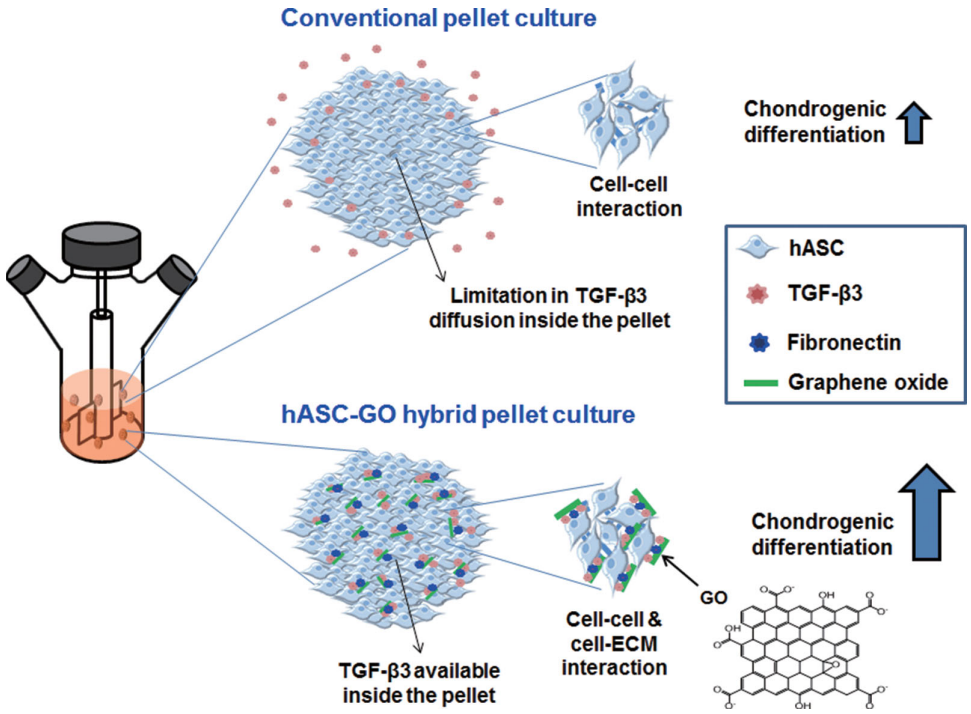

Figure 1. A schematic diagram describing the enhancement in chondrogenic differentiation of hASCs using GO. The conventional pellet culture provides only cell-cell interaction, and TGF-β3 diffusion inside the pellets is often limited; both of these factors limit the chondrogenic differentiation of stem cells. To improve chondrogenic differentiation, stem cells can be cultured in hybrid pellets of hASCs and GO. GO sheets are adsorbed with cell-adhesion proteins (e.g., FN) and TGF-β3 and dispersed in hASC pellets, providing cell-ECM interactions and TGF-β3 to enhance the chondrogenic differentiation of hASCs.

and carboxylic and hydroxyl groups. The π-electron clouds in the GO sheets are capable of interacting with the inner hydrophobic cores of FN and TGF-β3 proteins. These proteins can also be adsorbed through electrostatic interaction with the carboxylic and hydroxyl groups of GO. It was reported previously that hydroxyl groups strongly adsorb FN compared with other chemical groups.[13] Dispersion of FN- and TGF-β3-adsorbed GO sheets in hASC pellets may enhance chondrogenic differentiation of hASCs by adding a cell-FN interaction and supplying TGF-β3 effectively (Figure 1).

2. Results and Discussions

2.1. Characterization of GO Sheets

Figure 2A–C displays scanning electron microscopy (SEM), transmission electron microscopy (TEM), and atomic force microscopy (AFM) images of the as-synthesized GO sheets. The GO sheets had dimensions of approximately 0.5–1 μm (Figure 2C). Some of the GO sheets appeared to be self-folded (Figure 2A), indicating that the sheets were flexible. The TEM image and the corresponding electron diffraction (ED) pattern taken by directing the electron beam perpendicular to the flat faces of a GO sheet exhibited diffraction spots with a six-fold rotational symmetry, showing the graphene-like crystallinity of the GO (Figure 2B).[14] The AFM image analysis revealed that the GO sheets had a thickness of approximately 1.2 nm (Figure 2C). Additionally, to obtain a better understanding of the structure of the GO sheets, we conducted the Raman analysis. The characteristic peaks of the G band and D band taken from the as-synthesized GO sheets were 1590 cm^{-1} and 1350 cm^{-1} (I_D/I_G ratio of 1.07), respectively, which were similar to the literature values for GO (Figure 1D).[15,16]

2.2. GO Incorporation into hASC Pellets

To show GO incorporation into hASC pellets, SEM, TEM, and fluorescence microscopy images were acquired at day 1. In the SEM images, GO sheets were detected on the surface of the formed hybrid pellets (**Figure 3**A). To verify the GO distribution within the pellet, GO sheets were labeled with a fluorescent cationic dye, DiI, prior to incorporating them into the pellets. The acquired fluorescence images showed GO sheet dispersion throughout the formed pellets (Figure 3B). GO flakes at a concentration of 1 μg mL^{-1} may be hardly detectable. However, as the cells formed a pellet, the GO flakes (at 1 μg GO mL^{-1} cell-suspension volume) in the cell suspension were incorporated into the pellet and concentrated within the pellet by approximately 6 folds (GO concentration = 6 μg GO mL^{-1} pellet volume) as the pellet volume was approximately 6 folds less than the volume of cell suspension. Therefore, GO flakes in pellets (Figure 3B) were detectable as the concentration of GO flakes in the pellet would be much higher than 1 μg mL^{-1}. GO sheets are capable of quenching fluorescent dyes bound to GO sheet surface only at low concentrations of fluorescent dyes. It was reported that, at a GO concentration of 17 μg mL^{-1}, dye

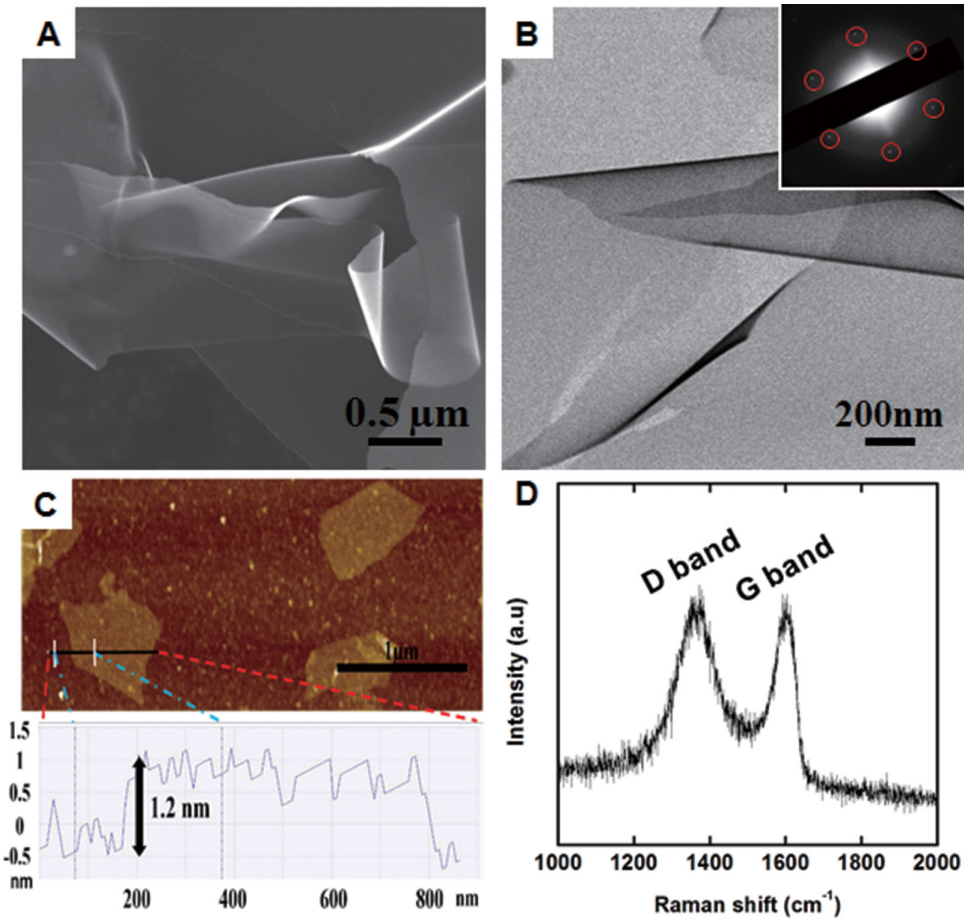

Figure 2. GO characterization. A) SEM image. B) TEM image and (inset) the corresponding ED pattern. C) Tapping-mode AFM image and the height along the line shown in the AFM image. D) Raman spectrum using 514-nm laser excitation.

fluorescence was observed only at dye concentrations higher than 1.5 μM. The non-quenching effect is due to the excessive dye accumulation on GO surfaces via electrostatic and/or π–π interaction. At dye concentrations lower than 1.5 μM, dye fluorescence quenching was observed.[17] Since the fluorescent dye concentration (6.25 mM) in this study was much higher than the reported threshold dye concentration (1.5 μM) and the GO sheet concentration (1 μg mL^{-1}) used was much lower, quenching could have been negligible and thus fluorescence was observed (Figure 3B and Figure S1, Supporting Information). TEM images revealed GO sheet interaction with hASCs in the hybrid pellets (Figure 3C).

2.3. Cytotoxicity of GO Sheets in hASC-GO Hybrid Pellets

To determine whether GO shows cytotoxicity, the viability and apoptotic activity of hASCs after GO sheet incorporation into the hybrid pellets were examined. Cell viability was assessed using fluorescein diacetate-ethidium bromide (FDA-EB) staining. FDA-EB staining indicated no cell death for either hASC pellets or hASC-GO hybrid pellets (**Figure 4**A). The apoptotic activity of hASCs was assessed with a terminal deoxynucleotidyl transferase dUTP nick end labeling (TUNEL) assay and by evaluating apoptotic gene and protein expression. Apoptotic cells were rarely detected with the TUNEL assay in any of the three groups of hASC pellets: pellets with TGF-β3 added to the medium (P+TGF-β), hybrid pellets of GO-hASCs with TGF-β3 added to the medium (P-GO+TGF-β), and hybrid pellets of GO-hASCs with TGF-β3-adsorbed GO sheets (P-GO-TGF-β) (Figure 4B). Reverse transcriptase polymerase chain reaction (RT-PCR) analysis revealed that the expression of apoptotic markers, caspase-3 protein and the *p53* gene did not show significant differences between groups (Figures 4C and D). These data clearly indicate no cytotoxicity of GO sheets prepared in this study. Cytotoxicity of GO has been reported previously.[18] In the previous study, GO sheets exhibit toxicity to hMSCs only at concentrations higher than 10 μg/ml and at a size range of 3.8 ± 0.4 μm. However, we used GO sheets at a concentration of 1 μg mL^{-1} with a size range of 0.5 to 1 μm in this experiment, and under these conditions, GO was non-toxic.

2.4. Chondrogenic Differentiation of hASCs

We investigated whether GO sheet incorporation into hASC pellets enhances the chondrogenic differentiation of the hASCs in vitro. The chondrogenic differentiation was examined

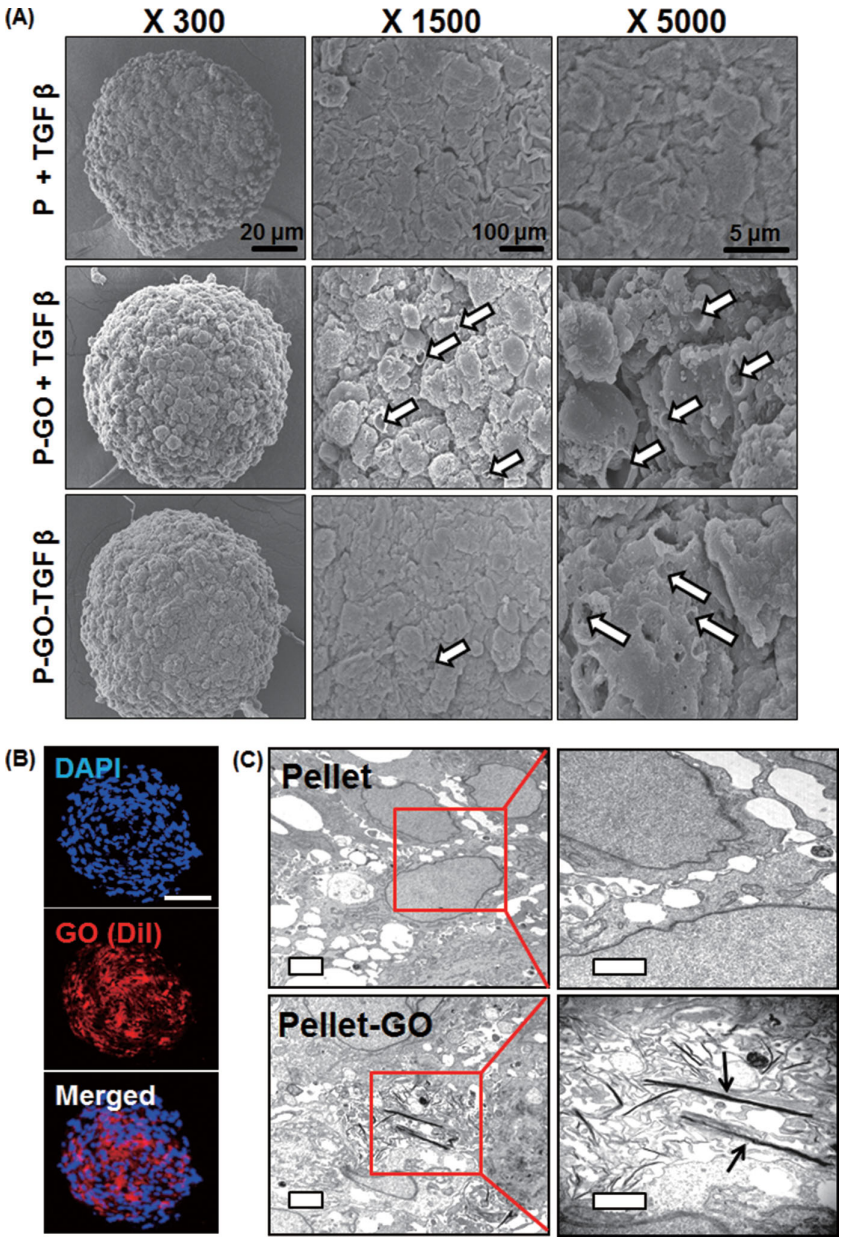

Figure 3. GO incorporation into hASC pellets. A) SEM images showing GO on the hybrid pellet surface (white arrows). P+TGF-β, hASC pellets with TGF-β3 added to the medium; P-GO+TGF-β, hybrid pellets of GO-hASCs with TGF-β3 added to the medium; P-GO-TGF-β, hybrid pellets of GO-hASCs with TGF-β3-adsorbed GO sheets. B) Distribution of DiI-labeled GO sheets (red) in the hybrid pellet. Scale bar indicates 100 μm. C) TEM images showing GO sheets (arrows) interacting with cells in the hybrid pellet. Scale bar indicates 0.5 μm.

by evaluating the expression of chondrocyte-specific ECMs (aggrecan, glycosaminoglycan, and type II collagen) and the transcription factor (SOX-9). The P-GO-TGF-β group showed a higher deposition of aggrecan compared with the other groups (**Figure 5**A). Deposition of type II collagen and glycosaminoglycan was also higher in the P-GO-TGF-β group (Figure 5B). Western blot analysis also confirmed a higher expression of type II collagen in the P-GO-TGF-β group (Figure 5C). RT-PCR and real-time PCR results indicated more extensive expression of chondrogenic genes in the P-GO-TGF-β group (Figure 5D). The P-GO+TGF-β group showed upregulation of SOX-9, a master regulator of chondrogenic differentiation compared with the P+TGF-β group. The expression was further increased in the P-GO-TGF-β group. During endochondral bone development, cells condense and form a cartilage template. Later, the template is terminally converted into bone by mineralization, which is called hypertrophic differentiation.[19] To determine whether the dispersion of FN- and TGF-β3-adsorbed GO sheets in hASC pellets affects hypertrophic differentiation, hypertrophic marker (collagen type X and RUNX2) expression was examined. At late stage of chondrogenic differentiation of ASCs, ASCs could undergo stages of cell hypertrophy and tissue mineralization which leads to bone formation.[20] Since the expression of hypertrophic markers was not different among all groups (Figure 5E), TGF-β3-adsorbed GO sheets did not promote hypertrophy of the ASCs.[21]

2.5. TGF-β3 Adsorption on GO

To explain the underlying mechanisms of the enhanced chondrogenic differentiation observed in the hybrid pellets, the protein structural stability of TGF-β3 adsorbed on the GO sheets was investigated. It was previously reported that the presence of oxygenated groups on GO can facilitate binding of proteins through electrostatic interactions.[5] In the study, insulin stably interacted with GO and induced adipogenic differentiation of hMSCs. Additionally, the authors showed, by circular dichroism (CD), preserved insulin structure on GO, whereas insulin lost its conformational structure on G. Thus, we hypothesized that GO sheets could stably adsorb TGF-β3 and, by introducing TGF-β3 directly to the cells in the hybrid pellets, could also avoid the diffusional limitation of TGF-β3 to the inner core of the pellets and enhance the chondrogenic differentiation of hASCs. TGF-β3 was stably adsorbed on GO, as evidenced by the negligible release of the protein from the GO sheets over 7 days evaluated with an enzyme-linked immunosorbent assay (ELISA) (**Figure 6**A). It was previously reported that hydrophobic and charged side chains of amino acids form π–π and electrostatic interaction with GO and does not dissociate readily. Since TGF-β contains all these amino acids within its sequence, the dissociation could have been negligible.[22] Also, TGF-β receptors are located on the surface of the cells and its interaction with TGF-β3 allows induction of cellular signaling cascade needed for chondrogenic differentiation.[23] Also, when cells interact with TGF-β3, they initiate molecular pathway to

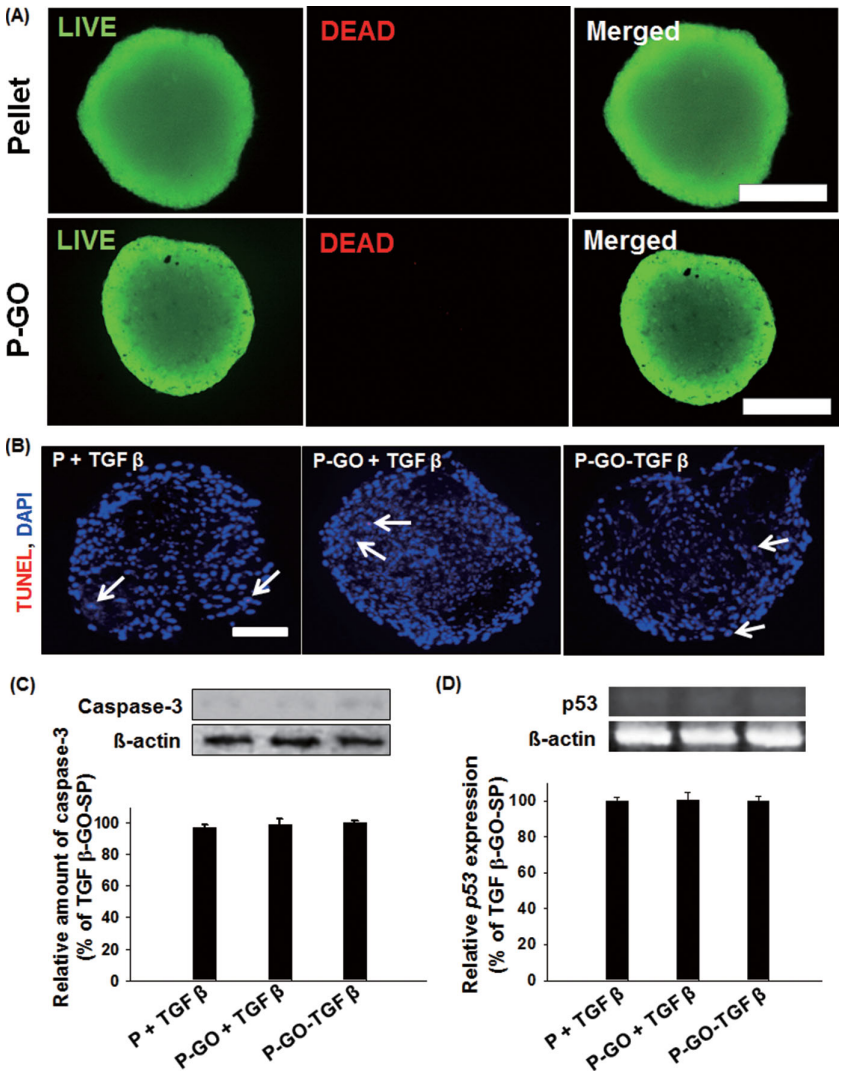

Figure 4. Cytotoxicity of GO sheets evaluated by the viability and apoptotic activity of hASCs in hybrid pellets of GO-hASCs. A) Viability of hASCs in hASC pellets (Pellet) and hybrid pellets of GO-hASCs (P-GO) evaluated with the FDA-EB assay, which stains live cells green and dead cells red. No red cells were observed in either group. Scale bar indicates 200 μm. B) The apoptotic activity of hASCs evaluated with the TUNEL assay, which stains apoptotic cells (white arrows) red. Blue (DAPI) indicates nuclei. Scale bar indicates 100 μm. The apoptotic activity of hASCs evaluated by C) western blotting for caspase-3 expression and D) RT-PCR of the *p53* gene expression (n = 3 for each group). There were no significant differences between any two groups.

enhance expression of TGF-β3 which are released from the cells and induces chondrogenic differentiation of the neighboring cells.[21] Next, we examined the structural stability of TGF-β3 adsorbed on the GO sheets by comparing the adsorbed structure with the structures of native TGF-β3 and TGF-β3 dissolved in the medium. CD analysis demonstrated that TGF-β3 closely retained its native structure when adsorbed on GO sheets more than when dissolved in the medium (Figure 6B). The enhanced structural stability of proteins adsorbed onto GO has been reported previously.[24] Additionally, it was previously reported that proteins are protected from enzymatic attack when bound to GO.[25] These data indicate that GO sheets are capable of adsorbing TGF-β3 and allowing TGF-β3 to retain its structure.

Efficient cellular accessibility of TGF-β3 in the hybrid pellets may also contribute to the enhanced chondrogenic differentiation. TGF-β3 distribution in the pellets was examined with immunostaining for TGF-β3. hASCs are capable of producing their own TGF-β3 under chondrogenic induction conditions.[21] To distinguish the TGF-β3 produced by hASCs from exogenous TGF-β3, mouse-originated TGF-β3 was adsorbed on GO sheets prior to pellet incorporation. The TGF-β3 adsorbed on GO sheets was dispersed throughout the hybrid pellets at 0 and 24 hours of pellet culture (Figure 6C and D). In contrast, when TGF-β3 was added to the culture medium, diffusion to the pellet inner core was limited, as evidenced by TGF-β3 detection only at the periphery of the pellet at 24 hours of pellet culture (Figure 6D). It is well known that the diffusional limitation of molecules such oxygen is approximately 150–200 μm in tissues.[12] Diffusional limitation of TGF-β3 in the pellets could limit the chondrogenic differentiation of hASCs in pellet cultures. Therefore, the preserved structure and efficient cellular accessibility of TGF-β3 adsorbed on GO sheets would contribute to the enhanced chondrogenic differentiation of hASCs.

2.6. FN Adsorbed on GO

To determine whether GO sheets can serve as a cell-adhesion substrate, cell-adhesion protein (e.g., FN) adsorption on GO sheets was examined. Following incubation of GO sheets in serum-containing medium, we performed energy-dispersive spectroscopy (EDS) and observed sulfur signals that were not present in GO, which confirmed protein adsorption on the GO sheets (**Figure 7**A). In addition, EDS mapping showed an even distribution of sulfur on the GO sheets. To determine FN adsorption on the GO sheets, proteins absorbed onto GO was extracted and western blot analysis was performed (Figure 7B). The results indicate that the proteins adsorbed on the GO sheets include FN. The FN adsorption on GO sheets is likely attributed to the FN interactions with the hydrophobic π domains and hydroxyl groups in the GO sheets. It was previously reported that hydroxyl groups have the strongest FN adsorption compared with amine, carboxyl, and methyl functional groups.[12]

2.7. Cell Signaling for Chondrogenic Differentiation

The higher protein stability and cellular accessibility of TGF-β3 and the provision of cell-FN interactions in the hASC-GO hybrid pellets promoted cell signaling responsible for chondrogenic

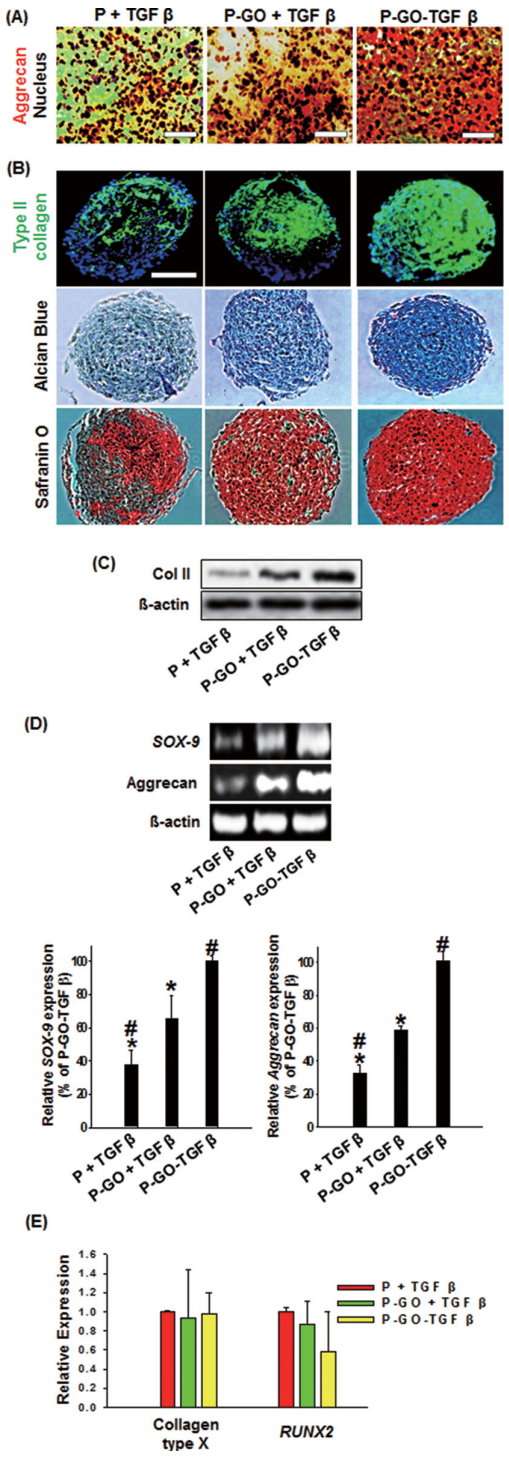

Figure 5. Enhanced chondrogenic differentiation in GO-hASC hybrid pellets at day 14. A) Immunocytochemical staining for aggrecan. Aggrecan and nuclei were stained brown and black, respectively. Scale bar indicates 30 μm. B) Immunocytochemical staining for type II collagen (green) and alcian blue and safranin O staining for glycosaminoglycan (blue and red, respectively). In staining for type II collagen, nuclei were counterstained with DAPI (blue). C) Western blot analysis for type II collagen. D) RT-PCR (top) and real time-PCR (bottom) analyses for chondrogenic markers. E) Real-time PCR analysis for hypertrophic markers. Scale bar indicates 100 μm (*$p < 0.05$ versus P-GO-TGF-β, #$p < 0.05$ versus P-GO-TGF-β, n = 3 for each group).

differentiation (**Figure 8**A). TGF-β initiates chondrogenic differentiation via activation of ERK, JNK, and p38.[26] When TGF-β3 was delivered via GO sheets, the phosphorylation (activation) of all three kinases, ERK, JNK, and p38, increased significantly compared with the other groups (Figure 8B). This was likely due to the stable and efficient delivery of TGF-β3 using GO in the hybrid pellets. In the P-GO-TGF-β group, the TGF-β3 structure was more stable, and the cellular accessibility of TGF-β3 was not limited inside the pellets (Figure 6B D). By contrast, when TGF-β3 was added to the medium, the activation of ERK, JNK, and p38 was significantly decreased compared with the activation when TGF-β3 was delivered via the GO sheets (Figure 8B). This was likely due to the rapid loss of the stable TGF-β3 protein structure in the medium and the diffusional limitation of TGF-β3 in the pellets (Figure 6B–D), which would, in turn, limit the chondrogenic differentiation of hASCs.

An additional aspect of the underlying mechanisms of the enhanced chondrogenic differentiation is the interaction between the cells and the FN absorbed on the GO. During early chondrogenesis, FN was reported to enhance cell condensation as well as differentiation of undifferentiated chondroprogenitors.[27] Upon cell interaction with FN, cells initiate chondrogenic differentiation in the region of the cell-FN interaction.[10,11,28] FN plays a functional role in the conversion of mesenchyme to chondroblasts, possibly through internal signaling provided by interaction between the $\alpha5\beta1$ integrin and the FN.[29] $\alpha5\beta1$ integrin is a FN receptor[30] and the most abundant $\beta1$-containing integrin in fetal cartilage.[31] When FN-adsorbed GO sheets were incorporated to hASC pellets, $\alpha5\beta1$ integrin expression was enhanced (Figure 8C), indicating a cell-FN interaction (Figure 8C). Thus, by providing FN as a cell-adhesion molecule (Figure 7B), GO sheets would have contributed to the promotion of chondrogenic differentiation of hASCs.[32]

The enhanced expression of chondrogenic markers in the P-GO+TGF-β group compared with the P+TGF-β group (Figure 5A-D) was likely due to the adsorption of FN on GO sheets. It is noted that FN was also expressed in the P+TGF-β group at day 1 of culture. This was likely due to the presence of TGF-β3 in the medium because TGF-β can induce FN synthesis.[33] However, the amount of FN was greater in the P-GO-TGF-β group, possibly due to the initial adsorption of FN on the GO (Figure 7) and the better cellular accessibility of TGF-β3 (Figure 6D).

GO may be advantageous to G in terms of chondrogenic differentiation of adult stem cells. It was reported that hydroxyl functional groups on GO surfaces have strong affinity for FN, which induces cellular expression of $\alpha5\beta1$ integrin that promotes chondrogenic differentiation, compared to other functional groups.[12] In contrast, it was reported that when MSCs adhered on G surfaces, they express focal adhesion kinase (FAK), which promotes osteogenic differentiation.[34] Also, it was reported that insulin proteins denature upon binding to G surface,[5] making it unsuitable for protein interaction and delivery in our study.

3. Conclusions

This study, for the first time, demonstrates the use of GO to promote chondrogenic differentiation of stem cells. Unlike

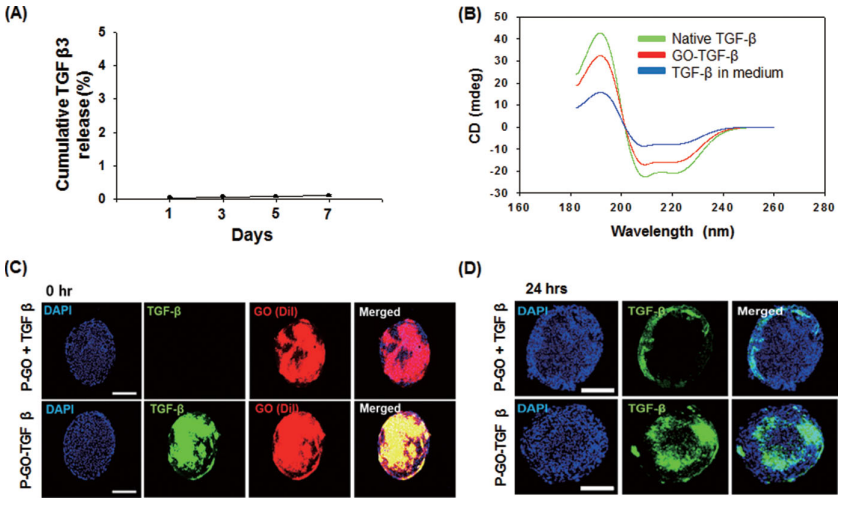

Figure 6. Protein structural stability and cellular accessibility of TGF-β3. A) Profile of TGF-β3 release from the GO sheets to the medium over 7 days showing stable adsorption on the GO sheets. B) CD analysis for evaluation of the protein structural stability of TGF-β3 on GO sheets. Immunostaining images and fluorescent images showing the distribution of TGF-β3 (green) adsorbed on GO sheets (red) in the pellet (blue; nuclei) at C) 0 h and D) 24 h after pellet formation. Mouse-originated TGF-β3 and an antibody against mouse TGF-β3 were used to distinguish it from the TGF-β3 that might be produced by hASCs. Scale bars indicate 150 μm in (C) and 100 μm in (D).

previous studies using G[5,6,8] or GO[5,7] as a culture substrate in two-dimensional (2D) monolayer culture system for stem cell differentiation, our study used GO as a protein-delivery carrier in a 3D culture system for stem cell differentiation. In conventional pellet culture for chondrogenic differentiation of stem cells, low cell-ECM interaction and the diffusional limitation of TGF-β may limit the chondrogenic differentiation of stem cells. In the present study, FN- and TGF-β-adsorbed GO sheets were incorporated into pellets of hASCs to provide a platform for cell-ECM interaction and to avoid the diffusional limitation of TGF-β, which resulted in significantly enhanced chondrogenic differentiation of hASCs. This study demonstrates that GO can be used to provide cell-adhesion signals and to supply a soluble factor effectively. The use of GO to promote chondrogenic differentiation of stem cells may open a new direction in tissue engineering and regenerative medicine.

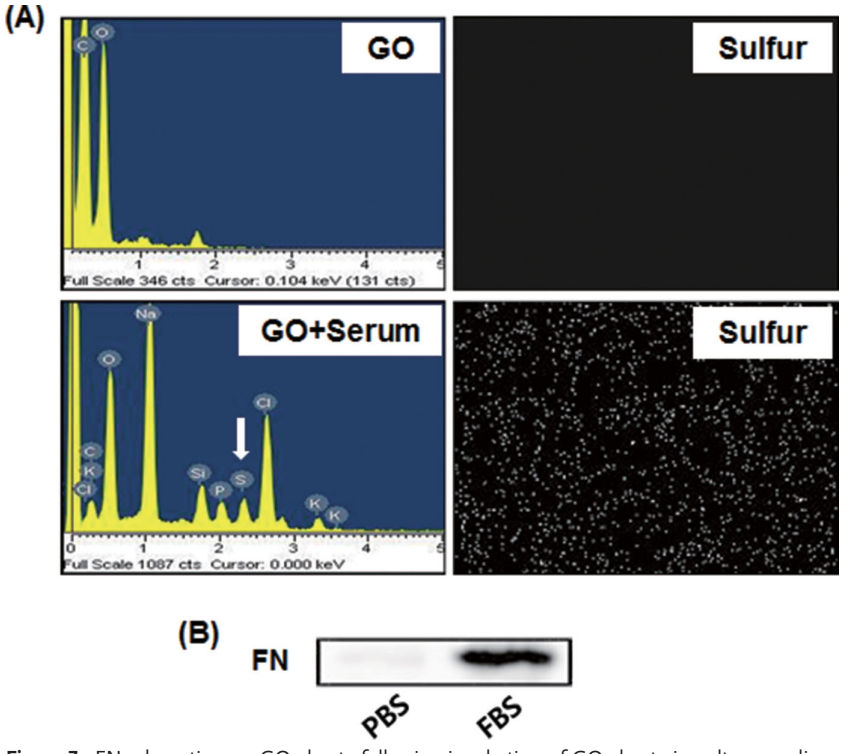

Figure 7. FN adsorption on GO sheets following incubation of GO sheets in culture medium containing 10% (v/v) serum for 4 hours. A) EDS analysis showing the adsorption of proteins from the serum on GO. The appearance of a sulfuric peak (arrow) and white dots indicate protein adsorption on the GO sheets. B) Western blot analysis demonstrating the adsorption of FN from serum on the GO sheets.

4. Experimental Section

GO Synthesis and Characterization: GO sheets were prepared as described previously using the modified Hummers method.[35] After synthesis, GO sheets were carefully separated by the centrifugation of the GO solution at 4000 rpm for 30 min three times, and then, the transparent brown upper solution of GO was collected.[36] Transmission electron microscopy (TEM) analysis was conducted with a JEOL JEM-2100F transmission electron microscope operating at 200 kV. Samples were prepared by putting a drop of the particle dispersions onto a carbon-coated copper grid. The surface morphology of the GO sheets was examined with field-emission scanning electron microscopy (FE-SEM) (JEOL JSM-6700F, SE resolution: 1.0 nm (15 kV), 2.2 nm (1 kV); Accelerating voltage: 0.5–30 kV). The sample topography and thickness measurements of the GO sheets were performed with a Nanoscope IIIA (Digital Instruments) atomic force microscope (AFM) in tapping mode. The Raman spectra of the samples were obtained with a Raman spectrometer (T64000) at room temperature, with an excitation laser source of 514 nm. EDS (INCA Energy, Oxford Instruments Analytical LTD., Bucks, UK) was used to identify and observe the protein absorption on the GO sheets following incubation of the GO sheets in 10% (v/v) serum-containing medium for 4 hours.

hASC Culture: hASCs were purchased from Lonza (Allendale, NJ, USA). hASCs were cultured in a growth medium consisting of α-minimum essential medium (α-MEM, Gibco BRL, Gaithersburg, MD, USA), 10% (v/v) fetal bovine serum (FBS, Gibco BRL), 100 units mL^{-1} of penicillin, and 100 μg/ml of streptomycin. hASCs at the fourth passage of cultivation were utilized for the experiments in this study.

hASC Pellet Formation and Chondrogenic Differentiation: To evaluate GO incorporation into hASC pellets, GO sheets were pre-labeled with DiI (6.25 mM, Invitrogen) at 4 °C for 6 hours and incorporated into pellets at 1 μg mL^{-1} concentration

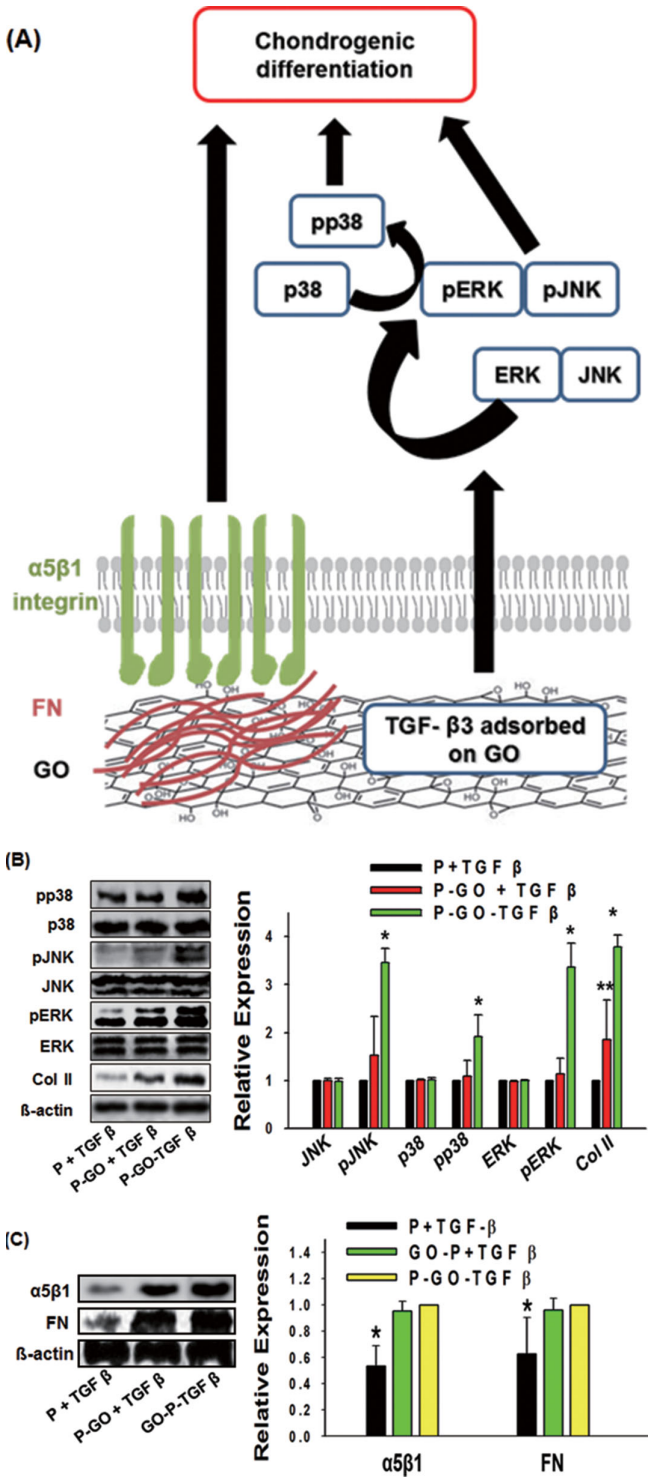

Figure 8. Cell signaling in the enhanced chondrogenic differentiation in the hASC-GO hybrid pellets. A) A schematic diagram of the underlying mechanisms describing the cell signaling induced by TGF-β3 and FN. B) Western blot analyses of the qualitative and quantitative expression of activated intracellular signaling molecules related to TGF-β3 signaling. (n = 3 per group, *$p < 0.05$ versus P + TGF-β, #$p < 0.05$ versus P-GO-TGF-β). C) Western blot analyses of the qualitative and quantitative expression of the $\alpha 5\beta 1$ integrin, a FN-binding integrin, and FN at day 1 of culture (n = 3 per group, *$p < 0.05$ versus P-GO-TGF-β3, **$p < 0.05$ versus P-GO+TGF-β).

for 24 hours. Briefly, GO was added to DiI solution and reacted for 6 hours at 4 °C. The solution was centrifuged at 13000 rpm and the supernatant containing unabsorbed DiI was discarded. The collected GO was gently washed twice with distilled water prior to use for pellet incorporation. To adsorb TGF-β3 first and FN second on GO sheets, GO sheets were suspended in distilled water containing TGF-β3 (600 ng) at a concentration of 1 μg/ml and incubated at 4 °C for 4 hours. Following the incubation, an ELISA preformed with the supernatant indicated that all TGF-β3 was adsorbed on the GO sheets. TGF-β3-adsorbed GO sheets were then incubated in α-MEM containing 10% (v/v) FBS for 4 hours to allow FN from the serum to be adsorbed on the GO sheets. GO sheets reacted only with α-MEM was used as another group. The hanging-drop method was used to form pellets as previously described[37] with a cell concentration of 3×10^6 cells mL^{-1} and a GO concentration of 1 μg mL^{-1} in the cell suspension. Conventional pellet culture without GO sheets was used as a control. After 24 hours of pellet formation, cell viability and apoptosis were evaluated using FDA-EB (Sigma) and a TUNEL assay kit (Millipore Corp., Billerica, MA). For the FDA-EB assay, pellets were incubated with a FDA-EB (5 μg mL^{-1} and 10 μg mL^{-1}, respectively) solution for 5 minutes at 37 °C and then washed three times with phosphate-buffered saline (PBS). Dead cells were stained red due to the nuclear permeability of EB. The viable cells, which are capable of converting the non-fluorescent FDA into fluorescein, were stained green. Formed pellets were transferred to spinner flasks (working volume = 100 ml, Wheaton, Millville, NJ, USA), which were siliconized with sigmacoat (Sigma, St. Louis, MO, USA) to prevent cell adhesion onto the flask walls before use. A chondrogenic medium consisting of Dulbecco's modified Eagle's medium high glucose (Gibco BRL), 50 mg mL^{-1} of ascorbic acid, and 100 nM of dexamethasone supplemented with 10 ng mL^{-1} of TGF-β3 (R&D systems, Minneapolis, MN, USA) was used, and cells were cultured at 40 rpm. For pellets containing TGF-β3-adsorbed GO sheets, TGF-β3 was not added to the chondrogenic medium. Medium was changed every other day for 14 days.

TEM Analysis: The pellets and hybrid pellets were fixed with Karnovsky's solution (EMS, Hatfield, PA, USA) for 24 hours at 4 °C and washed 3 times with a 0.05 M sodium cacodylate buffer. Then, the specimens were fixed with 2% osmium tetraoxide (sigma) for 2 hours at 4 °C, washed three times with cold distilled water, dehydrated through a series of graded ethanol (50, 60, 70, 80, 90, 95, 98, and 100%) and propylene oxide rinses, and finally embedded in Spurr's resin. The samples were then polymerized at 60 °C for 24 hours and cut into thin slices using an ultramicrotome (MTX, RMC, Arizona, USA). The thin sections were observed with a Libra 120 microscope (Carl Zeiss, Oberkochen, Germany).

SEM Analysis: The pellets and hybrid pellets were washed twice with PBS, prefixed with 4% (v/v) buffered glutaraldehyde (Sigma) for 1 hour, and fixed with 0.1% (v/v) buffered formaldehyde (Sigma) for 24 hours. The fixed specimens were dehydrated in ascending grades of ethanol, dried, and mounted on aluminum stubs. The specimens were subsequently coated with platinum using a Sputter Coater (Cressington 108, Cressington Scientific Instruments, Cranberry, PA, USA) and examined with SEM (JSM-6330F, JEOL).

Histology and Immunocytochemistry: Pellets were harvested on day 14. The specimens were fixed in 10% (v/v) buffered formaldehyde, dehydrated in a graded ethanol series, and embedded in paraffin. The specimens were sliced into 4-μm sections. The sections were stained with safranin O and alcian blue for glycosaminoglycan detection. The sections were also stained with anti-type II collagen and anti-TGF-β3 antibodies and counter-stained with 4,6 diamidino-2-phenylindole (DAPI, Vector Laboratories, Burlingame, CA, USA) for immunocytochemical analysis. Unless otherwise mentioned, all antibodies were purchased from Abcam (Abcam, Cambridge, UK). Aggrecan was detected using a human aggrecan antibody (Abcam). Staining was visualized with an avidin-biotin complex immunoperoxidase (Vetastain ABC kit, Vector Laboratories) and a 3,3′-diaminobenzidine (DAB) substrate solution kit (Vector Laboratories). Cell nuclei were counterstained with hematoxylin. All images were taken with a fluorescence microscope (Olympus IX 71, Olympus, Tokyo, Japan).

Table 1. Primer sequences for RT- and real-time PCR.

p53	Sense	5′-CGG GAT CCA TGG AGG AGC CGC AGT CAG AT-3′
	Antisense	5′-CCG CTC GAG TTT CTG GGA AGG GAC AGA AGA-3′
SOX-9	Sense	5′-GTA CCC GCA CTT GCA CAA C-3′
	Antisense	5′-TCG CTC TCG TTC AGA AGT CTC-3′
RUNX2	Sense	5′-GCA GCA CGC TAT TAA ATC CAA-3′
	Antisense	5′-ACA GAT TCA TCC ATT CTG CCA-3′
COLLAGEN X	Sense	5′-CCC TTT TTG CTG CTA GTA TCC-3′
	Antisense	5′-CTG TTG TCC AGG TTT TCC TGG CAC-3′
AGGRECAN	Sense	5′-ACC CTG GAA GTC GTG GTG AAA-3′
	Antisense	5′-CGT GGC AAT GAT GGC ACT G-3′

RT-PCR Analysis: Samples were lysed with TRIzol reagent (Invitrogen, Carlsbad, CA, USA). The total RNA was extracted with chloroform (Sigma) and precipitated with 80% (v/v) isopropanol (Sigma). After the supernatant was removed, the RNA pellet was washed with 75% (v/v) ethanol, air-dried, and dissolved in 0.1% (v/v) diethyl pyrocarbonate-treated water (Sigma). The RNA concentration was determined by measuring the absorbance at 260 nm with a spectrophotometer. Reverse transcription was performed with 5 μg of pure total RNA and SuperScriptTM II reverse transcriptase (Invitrogen) and was followed by PCR amplification of the synthesized cDNA. The primer sequences are shown in **Table 1**. The PCR consisted of 35 cycles of denaturing (94 °C, 30 sec), annealing (58 °C, 45 sec), and extension (72 °C, 45 sec), with a final extension at 72 °C for 10 min. The PCR was followed by electrophoresis on a 2% (w/v) agarose gel and DNA visualization by ethidium bromide staining. The PCR products were analyzed with a gel-documentation system (Gel Doc 1000, Bio-Rad, Hercules, CA, USA).

Real Time-PCR Analysis: Total RNA was extracted at day 14 using 1 ml of TRIzol reagent (Invitrogen) and 200 μl of chloroform. The samples were centrifuged at 12,000 rpm for 10 min at 4 °C. The RNA pellets were washed with 75% (v/v) ethanol and dried. After the drying procedure, the samples were dissolved in RNase-free water. The iQ SYBR Green Supermix kit (Bio-Rad Laboratories, Hercules, CA, USA) and the MyiQ single color Real-Time PCR Detection System (Bio-Rad Laboratories) were used. The primer sequences are shown in Table 1.

ELISA for TGF-β3: The profiles of the in vitro release of TGF-β3 from GO sheets were determined by ELISA (R&D Systems Inc., Minneapolis, MN, USA). TGF-β3-adsorbed GO sheets were placed in culture well inserts (Transwell, Corning) and immersed in PBS at 37 °C. At various time points, the supernatant was collected, and the TGF-β3 concentration in the supernatant was determined using the ELISA kit (n = 3 per group). Briefly, the capture antibody was diluted to the working concentration in PBS without the carrier protein, immediately placed on a 96-well microplate (Corning) and incubated overnight at room temperature. The supernatant was then aspirated, and each well was washed with wash buffer and blocked by adding reagent diluents (1% (w/v) of bovine serum albumin in PBS) to each well. After washing and adding the sample or standards to the plate, the detection antibody was added. Then, streptavidin-horseradish peroxidase was added to each well. Finally, the substrate solution was added to each well, and the 450-nm absorbance was read with a microplate reader (Powerwave, Bio-Tek, Winooski, VT, USA).

Circular Dichroism: The structure of TGF-β3 adsorbed on the GO sheets after incubation in PBS for 3 days was examined using CD (Jasco J-810, Applied Photophysics, Surrey, BA, UK) and compared with the structure of native TGF-β3 and TGF-β3 suspended in medium for 3 days. Total TGF-β3 was physically detached from the GO sheets followed by five freeze-thaw cycles at –70 °C and 37 °C. The total amount of TGF-β3 protein was quantified using the Bradford reagent (Sigma). Each CD spectrum and its corresponding high-tension voltage curve were recorded on a Jasco J-810 spectropolarimeter using a quartz cell with an optical path length of 1 mm. The scanning speed was set at 50 nm per minute, and the wavelength range was set at 160–280 nm.

Western Blot Analysis: Samples (n = 3 per group) were lysed in ice-cold lysis buffer (15 mM Tris HCl (pH 8.0), 0.25 M sucrose, 15 mM NaCl, 1.5 mM $MgCl_2$, 2.5 mM EDTA, 1 mM EGTA, 1 mM dithiothreitol, 2 mM NaPPi, 1 μg mL^{-1} pepstatin A, 2.5 μg mL^{-1} aprotinin, 5 μg mL^{-1} leupeptin, 0.5 mM phenylmethylsulfonyl fluoride, 0.125 mM Na_3VO_4, 25 mM NaF, and 10 μM lactacystin). The protein concentration was determined with a bicinchoninic acid (BCA) protein assay (Pierce Biotechnology, Rockford, IL, USA). Equal protein concentrations of each sample were mixed with sample buffer, loaded, and separated by sodium dodecyl sulfate-polyacrylamide gel electrophoresis (SDS-PAGE) on a 10% (v/v) resolving gel. The proteins that were separated by SDS-PAGE were transferred to an Immobilon-P membrane (Millipore Corp.) and were probed with antibodies (Abcam) against collagen type II, ERK, phosphorylated ERK (pERK), p38, phosphorylated p38 (pp38), JNK, and phosphorylated JNK (pJNK). β-actin served as the internal control. To detect FN adsorbed on GO, GO-coated titanium substrate was immersed in the serum-containing medium for 1 hour and washed 3 times with PBS. Then, the GO-coated titanium substrate was put in an ice-cold lysis buffer, and the absorbed proteins were scrapped from the GO. The buffer solution containing FN was transparent, indicating GO-free status of the sample. The sample was processed as described above for western blot analysis for FN.

Statistical Analysis: All quantitative data are expressed as the mean ± standard deviation. Statistical analysis was performed using ANOVA with a Bonferroni test. A *p*-value less than 0.05 was considered to be statistically significant.

Supporting Information

Supporting Information is available from the Wiley Online Library or from the author.

Acknowledgements

This study was supported by grants (2013036054 and 2013035745) from the National Research Foundation of Korea and the Korea Health 21 R&D Project, Ministry of Health and Welfare (H12C0199).

Received: March 11, 2014
Revised: June 9, 2014
Published online: August 22, 2014

[1] Z. Zhang, Z. Lu, Q. Zhao, J. Huang, H. Shen, Z. Zhang, *Small* **2011**, *7*, 460.
[2] K. P. Liu, J. J. Zhang, F. F. Cheng, T. T. Zheng, C. M. Wang, J. J. Zhu, *J. Mater. Chem.* **2011**, *21*, 12034.
[3] O. Akhavan, E. Ghaderi, H. Emamy, *J. Mater. Chem.* **2012**, *22*, 20626.
[4] K. Yang, J. Wan, S. Zjang, B. Tian, Y. Zhang, Z. Yiu, *Biomaterials* **2012**, *33*, 2206.
[5] W. C. Lee, C. H. Y. X. Lim, H. Shi, L. A. L. Tang, Y. Wang, C. T. Lim, K.P Loh, *ACS Nano* **2011**, *5*, 7334.
[6] S. Y. Park, J. Park, S. H. Sim, M. G. Sung, K. S. Kim, B. H. Hong, S. Hong, *Adv. Mater.* **2011**, *23*, H263.
[7] S. H. Ku, C. B. Park, *Biomaterials* **2013**, *34*, 2017.

[8] T. R. Nayak, H. Anderse, C. S. Makam, C. Khaw, S. Bae, X. Xu, P.-L. Ee, J.-H. Ahn, B. H. Hong, G. Pastorin, B. Ozyilmaz, *ACS Nano* **2011**, *5*, 4670.
[9] H. Afizah, Z. Yang, J. H. Hui, H. W. Ouyang, E. H. Lee, *Tissue Eng.* **2007**, *13*, 659.
[10] D. A. Frenz, N. S. Jaikaria, S. A. Newman, *Dev. Biol.* **1989**, *136*, 97.
[11] B. K. Hall, T. Miyake, *Bioessays* **2000**, *22*, 138.
[12] G. Mehta, A. Y. Hsiao, M. Ingram, G. D. Luker, S. Takayama, *J. Controlled Release* **2012**, *164*, 192.
[13] B. G. Keselowsky, D. M. Collard, A. J. Garcia, *J. Biomed. Mater. Res. A.* **2003**, *66*, 247.
[14] D. C. Marcano, D. V. Kosynkin, J. M. Berlin, A. Sinitskii, G. Sun, A. Slesarev, L. B. Alemany, W. Lu, J. M. Tour, *ACS Nano* **2010**, *4*, 4806.
[15] A. C. Ferrari, J. C. Meyer, V. Scardaci, C. Casiraghi, M. Lazzeri, F. Mauri, S. Piscanec, D. Jiang, K. S. Novoselov, S. Roth, K. Geim, *Phys. Rev. Lett.* **2006**, *97*, 187401.
[16] S. Stankovich, D. A. Dikin, R. D. Piner, K. A. Kohlhaas, A. Kleinhammes, Y. Jia, Y. Wu, S. T. Nguyen, R. S. Ruoff, *Carbon* **2007**, *45*, 1558.
[17] M. inoforoglu, B. Gur, M. Arik, Y. Onganer, K. Meral, *RSC Adv.* **2013**, *3*, 11832.
[18] O. Akhavan, E. Ghaderi, A. Akhavan, *Biomaterial* **2012**, *33*, 8017.
[19] E. J. Marckie, L. Ahmed, K.-S. Tatarczuch, C. M. Mirams, *Int. J. Biochem. Cell Biol.* **2008**, *40*, 46.
[20] K. Pelttari, A. Winter, E. Stech, K. Goetzke, T. Hennig, B. G. Ochs, T. Aigner, W. Richter, *Arthritis Rheum* **2006**, *54*, 3254.
[21] H. H. Yoon, S. H. Bhang, J.-Y. Shin, J. H. Shin, B.-S. Kim, *Tissue Eng.* **2012**, *18*, 1949.
[22] M. Zhang, B.-C. Yin, X.-F. Wang, B.-C. Ye, *Chem. Commun.* **2011**, *47*, 2399.
[23] M. Motoyama, M. Deie, A. Kanaya, M. Nishimori, A. Miyamoto, S. Yanada, N. Adachi, M. Ochi, *J. Biomed. Mater. Res. A.* **2010**, *92*, 196.
[24] W. G. La, S. Park, H. H. Yoon, G.-J. Jeong, T.-J. Lee, S. H. Bhang, J. Y. Han, K. Char, B.-S. Kim, *Small* **2013**, *9*, 4051.
[25] H. Shen, M. Liu, H. He, L. Zhang, J. Huang, Y. Chong, J. Dai, Z. Zhang, *ACS Appl. Mater. Interfaces* **2012**, *4*, 6317.
[26] R. Tuli, S. Tuli, S. Nandi, X. Huang, P. A. Manner, W. J. Hozack, K. G. Danielson, D. J. Hall, R. S. Tuan, *J. Biol. Chem.* **2003**, *278*, 41227.
[27] S. Ghosh, M. Laha, S. Mondal, S. Sengupta, D. L. Kaplan, *Biomaterials* **2009**, *30*, 6530.
[28] R. B. Widelitz, T. X. Jiang, *J. Cell. Physiol.* **1993**, *156*, 399.
[29] A. M. Delise, L. Fischer, R. S. Tuan, *Osteoarthritis Cartilage* **2000**, *8*, 309.
[30] M. A. Lan, C. A. Gersbach, K. E. Michael, B. G. Keselowsky, A. J. Garcia, *Biomaterials* **2005**, *26*, 4523.
[31] G. Hausler, M. Hemereich, S. Marlovits, M. Egerbacher, *Calcif. Tissue Int.* **2002**, *71*, 212.
[32] P. Singh, J. E. Schwarzbauer, *J. Cell Sci.* **2012**, *125*, 3703.
[33] B. S. Weston, N. A. Wahab, R. M. Mason, *J. Am. Nephrol.* **2003**, *14*, 601.
[34] M. Kalbacova, A. Broz, J. Kong, M. Kalbac, *Carbon* **2010**, *48*, 4323.
[35] M. S. Hummer, R. E. Offeman, *J. Am. Chem. Soc.* **1958**, *80*, 1339.
[36] B. G. Choi, Y. S. Huh, Y. C. Park, D. W. Hung, W. H. Hong, H. Park, *Carbon* **2012**, *50*, 5395.
[37] S. H. Bhang, S. Lee, J. Y. Shin, T. J. Lee, B. S. Kim, *Tissue Eng. Part A.* **2012**, *18*, 2138.